Induction of Scleroderma Fibrosis in Skin-Humanized Mice by Administration of Anti−Platelet-Derived Growth Factor Receptor Agonistic Autoantibodies

Arthritis & Rheumatology
DOI 10.1002/art.39728

Running head: Skin-humanized mice for scleroderma fibrosis.

Induction of scleroderma fibrosis in skin-humanized mice by anti-Platelet-Derived Growth Factor receptor agonistic autoantibodies

Michele M. Luchetti[1] MD, Gianluca Moroncini[1] MD PhD, Maria Jose Escamez[2] PhD, Silvia Svegliati Baroni[1] PhD, Tatiana Spadoni[1] PhD, Antonella Grieco[1] PhD, Chiara Paolini[1] PhD, Ada Funaro[3] PhD, Enrico V. Avvedimento[4] MD PhD, Fernando Larcher[2] PhD, Marcela Del Rio[2] PhD, Armando Gabrielli[1] MD.

[1]Dipartimento di Scienze Cliniche e Molecolari, Clinica Medica, Università Politecnica delle Marche, Ancona, Italy; [2]Epithelial Biomedicine Division, CIEMAT-CIBERER (U714)/Department of Bioengineering, UC3M/Instituto de Investigaciones Sanitarias dela Fundacion Jimenez Diaz (IIS-FJD), Madrid, Spain; [3]Dipartimento di Scienze Mediche, Università di Torino, Turin, Italy; [4]Dipartimento di Medicina Molecolare e Biotecnologie Mediche, Università Federico II, Naples, Italy.

Acknowledgement This work was supported by Fondazione Medicina Molecolare e Terapia Cellulare (research funding to the Università Politecnica delle Marche, Ancona, Italy), and grants from Ministero Italiano per l'Università e la Ricerca Scientifica (to Drs. Avvedimento, and Gabrielli), AIRC IG /11364 and Epigenomics Flagship Project—EPIGEN/C.N.R. (to Dr Avvedimento), Ministero Italiano della Salute RF-2011-02352331 (to Dr Gabrielli), and grants PI14/00931 and S2010/BMD-2359 (to FL) and SAF 2013-43475-R and S2010/BMD2420 (to MDR)

Drs. Moroncini, Svegliati Baroni, Avvedimento, and Gabrielli hold a patent application (US Patent Application no. 13/812,764; Epitopes of the human PDGF Receptor able to bind human autoantibodies, antibodies and uses thereof). Dr. Gabrielli has received consulting fees, speaking fees, and/or honoraria from Actelion Pharmaceuticals (less than $10,000).

Address correspondence to: Armando Gabrielli, MD Dipartimento di Scienze Cliniche e Molecolari, Clinica Medica, Università Politecnica delle Marche, Via Tronto 10/A, 60126, Ancona, Italy. Tel: (39) 0712206101. Fax: (39) 2206103. Email: a.gabrielli@univpm.it

ABSTRACT

Received: Jul 09, 2015; Revised: Feb 10, 2016; Accepted: Apr 19, 2016

Objective Here, we report a skin-SCID mouse chimerical model for Systemic sclerosis (scleroderma, SSc) fibrosis based on the engraftment of *ex vivo* bioengineered skin using skin cells derived either from scleroderma patients or healthy donors.

Methods Tri-dimensional bioengineered skin containing human keratinocytes and fibroblasts isolated from skin biopsies of healthy donors or SSc patients, was generated *ex vivo* and then grafted onto the back of severe combined immunodeficiency (SCID) mice. The features of skin grafts were analyzed by immunohistochemistry and the functional profile of the graft fibroblasts was defined before and after treatment with IgG from healthy controls or SSc patients. To demonstrate the involvement of PDGFR: i) Nilotinib, a tyrosine kinase inhibitor was administered to mice before injection of SSc-IgG into the grafts; ii) human monoclonal anti PDGF receptor (PDGFR) antibodies were injected into the grafts.

Results Depending on the type of bioengineered skin grafted, the regenerated human skin presented either the typical scleroderma phenotype or the healthy human skin architecture. Treatment of animals carrying healthy donor skin grafts with SSc-IgG resulted in the appearance of *a bona fide* scleroderma phenotype as confirmed by the increased collagen deposition and fibroblasts activation markers. Administration of Nilotinib and the experiments with the monoclonal antibodies confirmed the involvement of PDGFR.

Conclusions This is the first demonstration *in vivo* of the fibrotic properties of anti-PDGFR agonistic antibodies. Furthermore, this bioengineered skin-humanized mouse model can be used to test *in vivo* the progression of the disease and to screen for anti fibrotic drugs.

Systemic Sclerosis (Scleroderma, SSc) is a disorder of the connective tissue characterized by fibrosis of the skin, and visceral organs (1,2). Additional manifestations include alterations of the microvasculature and production of auto-antibodies. The disease progression and severity vary greatly among SSc patients with death occurring due to end-stage organ failure. Scleroderma fibrosis is caused by an excessive deposition of type I collagen in the extracellular matrix (ECM) maintained by a persistent activation of dermal fibroblasts (3). Human dermal fibroblasts isolated from skin biopsies of SSc patients can be cultured *in vitro* and grown as monolayer onto plastic surfaces, where they retain SSc-like features, such as the increased expression of type I collagen genes (4), for several passages, after which they lose the SSc-like phenotype (5). Previous work demonstrated that one of the mechanisms underlying this persistently activated SSc fibroblast phenotype *in vitro* consists in a self-maintaining intracellular loop linking increased production of reactive oxygen species (ROS) (6,7), stabilization of up-regulated Ha-Ras (8), and phosphorylation of ERK1/2. The most immediate explanation for the loss of such phenotype after some passages *in vitro* can be ascribed to the absence, under standard cell culture conditions, of circulating stimulatory factors, that are present *in vivo* in SSc patients (9-14).

To replicate these mechanisms *in vivo*, we took advantage of a methodology developed to generate *ex vivo* large tri-dimensional bioengineered skin, using human keratinocytes and fibroblasts isolated from small skin biopsies, expanded and grown *in vitro* (15,16), then engrafted onto the back of several severe combined immunodeficiency (SCID) mice, which lacking humoral and cell-mediated immunity can be used as recipients of xenografts. Such skin equivalents are composed only by human keratinocytes and fibroblasts. Tissue vascularization during engraftment and

remodeling occurs exclusively from the host as previously demonstrated (17). This information is relevant in this study, because we can discriminate the effects of the autoantibodies on the human-specific PDGF receptor (PDGFR) from the effects on endothelial cells of the host.

This skin-humanized mouse model has already been employed to interrogate the molecular and cellular mechanisms of wound healing (18), immune-mediated disease processes (17), and several genodermatoses (19-21).

In this study, we describe the successful application of this method in developing two novel chimerical mouse-human models of SSc fibrosis. The first one was obtained after engraftment of bioengineered skin carrying SSc cutaneous cells onto immunodeficient mice. The second model was generated by injecting *in vivo* SSc-IgG into the engrafted bioengineered skin carrying healthy donor cutaneous cells.

Patients and Methods

Cell cultures

Primary keratinocytes and fibroblasts were isolated from skin biopsies obtained from 3 SSc patients (Supplemental Table 1) and 3 healthy controls (HC) after informed consent and the approval of the study protocol by the Institutional Ethics Committee of Università Politecnica delle Marche by enzymatical digestion with trypsin (0.05%)/ ethylenediaminetetraacetic acid (EDTA, 0.02%) (T/E). Cells were grown in Dulbecco's modified Eagle's medium DMEM/HAM-F-12 medium supplemented with 10% FCS, epidermal growth factor, insulin, cholera toxin, hydrocortisone, triiodo-thyronine, and adenine as previously described, in the presence of $2x10^6$ lethally irradiated 3T3-J2 cells and cultured as described (15,16). The remaining tissue was further digested in collagenase solution (Type I, 2 mg/mL) (Sigma, St. Louis, MO) to obtain primary fibroblast cultures grown in high glucose (1g/liter) DMEM supplemented with 10% FCS. Human keratinocytes and fibroblasts that have undergone at least 2 passages in culture were used for the preparation of the bioengineered skins. The presence of CD19+, CD3+, CD34+ and CD14+ contaminating cells was ruled out by FACS analysis.

Preparation of *ex vivo* bioengineered skins

A plasma scaffold populated with autologous fibroblasts (either from normal or SSc donors) was used as the dermal component of the bioengineered skin. Fresh frozen plasma was obtained from voluntary HC of the local blood bank and the plasma-based dermal equivalent prepared as follows: 6 to $7.5x10^4$ cultured fibroblasts were resuspended in 10 ml of plasma containing 10 mg of tranexamic acid (antifibrinolytic agent, Amchafibrin, Fides-Ecofarm, Barcelona, Spain) to strengthen the hydrogel and reduce the degradation of the fibrin due to fibrinolytic activity of growing dermal human

fibroblasts embedded in the scaffold. The final volume was, then, adjusted to 23 ml by adding 0.9% NaCl, and, finally, 2 mL of 1% $CaCl_2$. The mixture was placed in a tissue culture flask (75 cm^2) and let clot into a tri-dimensional hydrogel at 37°C in a CO_2 incubator for 30 minutes.

Keratinocytes (either from normal or SSc donors) were seeded on the plasma-fibroblast dermal equivalent either at 8 to 9 x 10^4 cells/cm^2 and after approximately 1 week the bioengineered skin was ready for engrafting.

Nine bioengineered skins were obtained from each skin biopsy and each one was grafted on the back of an immunodeficient mouse (27 mice with SSc skin grafts and 27 mice with HC skin grafts).

Animals and experimental engrafting protocol

Immunodeficient Rj: NMRI—Foxn1nu (NMRI nu) (SCID) mice (6–8 weeks old) were used (Elevage Janvier, Le Genest Saint Isle, France). Mice were housed for the duration of the experiments at the CIEMAT Laboratory Animals Facility (Spanish registration number 28079-21A) in pathogen-free conditions using micro-isolators, individually ventilated cages type IIL, at a maximum of six mice per cage, with 25 air cage changes per hour, in heat-treated soft wood pellets beds. All experimental procedures were carried out according to the European and Spanish laws and regulations on the protection and use of animals in scientific research (European Convention 123, Spanish R.D223/88 and O.M13–10–89 of the Ministry of Agricultural, Food and Fisheries, animal protection biosafety and bioethics guidelines). Procedures were approved by the local Animal Experimentation Ethical Committee according to all external and internal biosafety and bioethics guidelines. Each plasma-based bioengineered skin was fixed to a non-petroleum gauze with an inorganic polymer

glue (Histoacryl, B/Braun Aesculap, Tuttlingen, Spain), manually detached from the culture flask and then placed orthotopically on the back of one SCID mouse under sterile conditions as previously described (15). Mice were anesthetized before creating a full-thickness 3 cm^2 wound on the dorsum that matched a 3 cm^2 equivalent piece of skin cut from the 75 cm^2 scaffold. Devitalized mouse skin was used as a biologic bandage to protect and hold the skin substitute in place during the take process. Mice were observed daily and 8 weeks post grafting were injected with IgG or PBS as described below. At the appropriate experimental time points, mice were anesthetized by exposure to 3% v/v isofluorane in medical oxygen, and the human skin grafts were surgically removed.

Purification and injection of SSc-IgG

IgG were purified from sera of 8 SSc patients (SSc-IgG) (Supplemental Table 2) and 8 healthy controls (HC-IgG) using gravity flow columns (Pierce) as described (12). IgG from 8 SSc patients, which stimulated collagen production in normal fibroblasts *in vitro* through the PDGFR and IgG from 8 healthy subjects were independently merged into two distinct pools prior to stimulation experiments. For these experiments, nine bioengineered skins were obtained from each of 4 healthy donor skin biopsy (36 HC skin grafts), and each skin graft was engrafted on the back of one SCID mice (36 mice). 1 cm^2 area of the HC skin grafts was tattooed and injected with 100 μl (20μg) of purified SSc-IgG, or HC-IgG, at a concentration of 200 μg/ml, at days 0, 3, 6, and 9. PBS, 100 μl, was used as vehicle control. The three experimental conditions were each applied to 12 mice engrafted with the HC regenerated skins. Three mice for each condition were sacrificed at week 2, 4, 8, and 12 after the first injection, which was administered 8 weeks after grafting.

Human monoclonal anti PDGF receptor antibodies

In a further set of experiments with *ad hoc* prepared HC skin grafts, 2 μg of human monoclonal anti PDGFR antibodies V_HPAM-V_κ16F4 and V_HPAM-V_κ13B8, generated as described (14), were each injected at days 0, 3, 6, and 9, in 3 HC skin grafts using PBS and SSc-IgG as negative and positive control, respectively.

Nilotinib treatment protocol

Sixteen weeks after the HC bioengineered skin grafting, 16 mice were treated either with nilotinib (n=8) or the vehicle (n=8). Nilotinib (kindly provided by Novartis, Basel, Switzerland) was administered by oral gavage at a dosage of 75 mg/kg once a day for 42 days using a stainless steel straight feeding needle (24 gauge, 25.4 mm, PANLAB SL). A suspension of nilotinib at a concentration of 8 mg/ml was prepared daily by adding the vehicle, an aqueous solution composed of 0.5% hydroxypropylmethylcellulose (HPMC, Sigma 423181) and 0.05% Tween 80 (Sigma P 1754). After 30 days of treatment, SSc-IgG or HC-IgG were each injected into four mice in each experimental group (nilotinib-treated or vehicle-treated) as described above, and mice were sacrificed at day 42 (30+12).

Histopathological analysis

For evaluation of dermal thickness in skin grafts, sections were stained with haematoxylin-eosin (H-E) and observed under light microscopy (Olympus) at 200X magnification, and the distance between the epidermal–dermal junction and the dermal–subcutaneous fat junction was measured. Dermal thickness in SSc skin grafts and SSc-IgG-treated HC skin engrafts was calculated as fold increase in comparison with the corresponding controls.

Evaluation of microvessels in skin grafts

Sections were deparaffinised, rehydrated and stained with anti CD31 primary antibody (1 :400, Abcam, Cambridge, UK) overnight at 4°C and incubated with goat anti-mouse biotinylated antiserum (Thermo Scientific, Fremont, Ca, USA) for 10 minutes at room temperature. The peroxidase ABC method was performed using diaminobenzedine hydrochloride (DAB) as chromogen (Thermo Scientific). In each section, CD 31 positive vessels were counted in three randomly chosen fields.

Determination of ROS, Ha-Ras and pERK-1/2

Intracellular ROS generated by adherent fibroblasts were determined using 2',7'-dichlorofluorescein diacetate (DCFH-DA) as a probe as described (6).

Fibroblasts isolated from skin grafts and from skin biopsies were lysed and processed as described (6). Ras proteins were immunoprecipitated overnight at 4°C with polyclonal anti-pan Ras antibody and agarose-Protein A/G (Santa Cruz Biotechnology), and subjected to SDS-PAGE followed by transfer onto polyvinylidene fluoride (PVDF) membranes. For p-ERK, protein extracts (30 µg) were separated on 4-12% SDS-PAGE and transferred to PVDF membranes and probed with anti-Ha-Ras or anti-pERK-1/2 antibodies (1:1000, Santa Cruz Biotechnology) overnight at 4°C. After incubation with the appropriate HRP-labeled secondary antibodies for 1 hour, signals were detected with ECL Western Blotting Detection reagents (Amersham Bioscience).

Statistical analysis

All data were quantified as means ± standard deviation (SD). A two-tailed Student's t-test was applied to compare the means of samples using GraphPad Prism 4.0 (San Diego, CA). Differences were considered statistically significant when $P<0.05$.

Results

SSc skin grafts transiently retain their phenotype *in vivo*

Keratinocytes and fibroblasts were isolated from forearm skin biopsies of 3 SSc patients and 3 HC, cultured in vitro, and assembled into tri-dimensional bioengineered skins for each donor, which were then independently grafted onto the back of a corresponding number of immunodeficient mice. A total number of nine mice for each skin donor, to generate a SSc skin-humanized mouse or HC skin-humanized mice. Skin grafts as well as their dermal fibroblasts were analysed after engraftment at week 8, 12, 16 and 24. Fibroblasts grown from the original skin biopsies were used as a further control.

Eight weeks after grafting, picrosirius red staining showed the presence of a dense collagenous dermal tissue in the SSc skin grafts which was much less represented in the HC skin grafts (Fig. 1 A and Fig 1B $p<0.001$). Fibrosis of the SSc skin grafts was similar to that observed in skin biopsies from the same SSc patient from which they were derived (data not shown).

In agreement with our previous report (6), levels of Ha-Ras and pERK-1/2 were significantly higher in fibroblasts grown from SSc skin biopsies than in fibroblasts from HC biopsies (Fig.1C). and, 8 weeks after engrafting, in fibroblasts from the SSc skin grafts than in those obtained at the same time point from HC skin grafts (Fig.1C). Consistently, ROS production and COL1A2 gene expression were also significantly higher in fibroblasts from the original SSc skin biopsy than in HC fibroblasts (453.16 ± 40.41 vs 191.83±22.57 for ROS $p< 0.01$ and 3.08±0.65 fold increase relative to HC SB for collagen, $p<0.01$) (Fig.1D). and in fibroblasts taken from the SSc and HC skin grafts 8 weeks after engrafting (389.50±36.85 vs 253.33±33.26 for ROS $p<0.01$ and

2.05 ± 0.44 fold increase relative to HC SG for COL1A2, $p<0.01$) (Fig. 1D).

The SSc features were retained up to 16 weeks after engrafting, when levels of the aforementioned fibrotic biomarkers decreased in SSc grafts but still significantly higher than in the fibroblasts grown from the original SSc skin biopsies or in the 6 HC skin grafts (data not shown). Twenty-four weeks after engraftment both the SSc grafts and the SSc fibroblasts in culture became undistinguishable from normal HC grafts (data not shown).

These data demonstrate that the human skin-SCID mouse we present faithfully replicates the SSc fibrotic phenotype *in vivo*. However, we note that akin to fibroblasts growing in culture, SSc regenerated skin gradually lost disease markers and became undistinguishable from the skin derived from healthy donors, The transient nature of the *ex vivo* SSc fibrosis indicate that the continuous presence of factor(s) in trans, such as SSc-IgG, is required to maintain the SSc phenotype.

IgG purified from serum of SSc patients induce dermal fibrosis *in vivo*

Previous studies demonstrated that the serum of SSc patients contains stimulatory autoantibodies inducing the increase of collagen gene transcription in fibroblasts *in vitro* (11, 13). In order to replicate this finding *in vivo*, skin-humanized mice produced after grafting of bioengineered skin from 4 healthy donors were injected 8 weeks after grafting with 20 μg of purified serum IgG taken from a pool of eight SSc patients (12 mice), or from a pool of eight healthy controls (12 mice), or with PBS (12 mice) every three days in the dermis of the HC skin grafts. Unlike the skin-humanized mice injected with HC-IgG, those injected with SSc-IgG displayed significant dermal collagen accumulation 2 weeks after the first injection (Fig. 2A). Thus, dermal fibrosis became evident after four SSc-IgG injections and lasted for 12 weeks, as

demonstrated by sequential collagen quantification of the engrafted skins (data not shown).

Compared to fibroblasts obtained from skin-humanized mice injected with HC-IgG, the fibroblasts grown from biopsies of the grafts taken 2 weeks after the first SSc-IgG injection, exhibited higher levels of Ha-Ras and pERK-1/2 (Fig. 2B), produced increased amount of ROS compared to HC-IgG and PBS (458 ± 51 vs 238 ± 45 and 182±54, respectively; $p<0.01$) (Fig. 2C), and showed higher COL1A2 gene expression (2.2±0.54 vs 1.0±0.14 and 1.0±0.13 fold, respectively $p< 0.01$) (Fig. 2C).

Moreover, the staining for CD31, a marker of endothelium vessels, showed a marked decrease of the number of dermal vessels by SSc-IgG (8±2 vs 21±3 and 20 ± 2 $p< 0.01$ respectively) (Fig. 2D).

These results demonstrate that SSc-IgG, but not HC-IgG, activated normal fibroblasts *in vivo* in a manner that faithfully replicated the histological and molecular features of SSc skin grafts and with activation of the Ha-Ras-pERK-1/2-ROS loop and with vessel desertification.

SSc-IgG induce dermal fibrosis in vivo through PDGF receptor signalling

To demonstrate that dermal fibrosis is induced *in vivo* by SSc-IgG via PDGFR, normal human fibroblasts depleted of both PDGFR α and β chains were prepared from healthy donors by stable transduction with retroviral vectors encoding PDGFR-specific short-hairpin-RNAs (sh-RNAs). The downregulation of PDGFR α and β expression in the fibroblasts was assessed by FACS analysis and immunoblotting (Supplemental Fig. 1 A, B), and was consistently confirmed by the reduced *in vitro* response of fibroblasts to SSc-IgG, indicated by absence of Ha-Ras increase (Supplemental Fig1C) and COL1A2 gene induction (Supplemental Figure 1D). However, these

modified fibroblasts impaired the formation of the bioengineered skin because the human fibroblasts with PDGFR knocked-down were unable to sustain a stable keratinocyte/fibroblast scaffold in vitro (23). Thus, an alternative approach to generate a PDGFR-knockout regenerated skin was employed using mouse embryo fibroblasts derived from PDGFR-knockout embryos (F-/-). However, these modified bioengineered skins onto the back of immunodeficient mice induced skin cancer after 3 weeks, likely caused by reactivation of the Epstein-Barr virus used to immortalize F-/- cells (data not shown).

To circumvent these problems, a different experimental strategy was employed based on the administration of nilotinib, a tyrosine kinase receptor inhibitor (TKI) (24), to mice before the injection of SSc-IgG into the normal skin humanized mice. Nilotinib administration prevented accumulation of extracellular matrix and reduced skin thickness (Fig.3 A, B), and collagen (Fig. 3C, D) in all of the 8 mice treated with SSc-IgG, demonstrating that the increased collagen deposition induced by SSc-IgG involves the PDGFR activation. Moreover, observation of picrosirius red-stained skin sections under polarized light showed that SSc-IgG induced alteration of the architecture of extracellular matrix collagen as in SSc patients (25), characterized by increased reddish birefringence revealing thick parallel collagen bundles longitudinally aligned, typical of fibrotic processes (Fig.3D) (26). In contrast, in nilotinib treated mice, amelioration of the SSc phenotype was demonstrated by the presence of a weak, orange-yellowish birefringence of less dense, randomly oriented collagen fibers, in the dermis similar to that occurring in HC-IgG treated mice (Figure 3 D). Interestingly, in nilotinib treated mice a reduction of dermal vessel desertification induced by SSc-IgG was documented (Fig. 4 A, B).

The inhibition of fibrosis by nilotinib may be ascribed to mechanisms which do not involve PDGFR. In fact, besides PDGF, TGFβ also has a complex signaling cascade which includes tyrosine kinases amenable to blockade using TKIs (27). Furthermore, the chemical proteomic profile of nilotinib revealed that a nonkinase target, such as the oxidoreductase quinone reductase 2 (NQO2) which contributes to superoxide generation (28), is also inhibited by the drug.

Thus, to confirm that the activation of fibrosis *in vivo* by autoantibodies occurs through PDGFR, HC skin-humanized mice were injected with human monoclonal anti PDGFR antibodies generated from SSc B cells as described by Moroncini et al (14). Human monoclonal anti PDGFR antibody V_HPAM-V_κ16F4, which binding and stimulating the receptor induces the scleroderma phenotype in normal human fibroblasts *in vitro* (14), induced fibrosis *in vivo* when compared to V_HPAM–V_κ13B8, which binds but does not stimulate the receptor *in vitro* (14), as demonstrated by morphometric analysis of picrosirius staining of the HC skin grafts (139 $\pm$ 20 vs 97 $\pm$ 15 respectively $p< 0.01$) (Fig 5A), and COL1A2 gene expression in the skin grafts (3.6 $\pm$ 0.5 vs 1.05 $\pm$ 0.25 and 1 $\pm$ 0.3 respectively $p< 0.01$) (Fig. 5B). The administration of V_HPAM-V_κ16F4 was also responsible for reduced number of CD31 positive vessels in the grafts when compared to V_HPAM-V_κ13B8 (8 $\pm$ 3 vs 24 $\pm$ 5 respectively $p<0.01$) (Fig. 5C).

Taken together, these data imply that agonistic anti-PDGFR autoantibodies present in the serum of SSc patients induce fibrosis *in vivo.*

Discussion

Understanding of SSc pathogenesis has benefited from the study of tissue fibrosis in experimentally induced, naturally occurring, or genetically engineered animal models (29,30). However, the mouse skin and human are different and the mouse models available so far do not recapitulate the complex phenotype of SSc skin fibrosis. Aim of the present work was to contribute to this vital area of SSc research by creating a human regenerated skin-SCID mouse chimera with the specific intent of validating the pathogenic contribution of stimulatory PDGFR autoantibodies to dermal fibroblasts activation *in vivo*.

Ex vivo bioengineered skins have already been employed for different goals (17-21). The protocol involves the isolation, expansion and growth of human keratinocytes and dermal fibroblasts in order to *ex vivo* engineer a graftable tri-dimensional skin equivalent, which, upon engraftment onto the back of immunodeficient mice become vascularized by the host tissue. There are several advantages with using *ex vivo*-bioengineered skins. First, *in vitro* expansion of the cells allows generating large sheets of bioengineered skin from a single human skin biopsy, thus reducing the total number of skin biopsies needed and, more relevant, the experimental variability among the engrafted mice, with a clear advantage in terms of experimental standardization over mice engrafted with individual skin samples. Second, expression of relevant genes can be manipulated *ex vivo*. Third, skin grafts remain histologically distinct within the host tissue.

The skin-humanized mice described herein provided very relevant information. First, fibroblasts and keratinocytes cultured from SSc skin biopsies retained their pathologic phenotype when used to build the regenerated skin *in vivo*. However, like scleroderma

fibroblasts in culture (5), SSc bioengineered skins engrafted onto the back of immunodeficient mice gradually lost disease markers (i.e.: ROS and collagen overproduction) and became undistinguishable from those generated from healthy donor cells. This finding indicates that SSc fibroblasts and keratinocytes do not display any type of constitutive defect and suggests that additional factors absent in the engrafted skin, and also in the host mouse tissue, are required to maintain the SSc phenotype.

Our working hypothesis was that such additional factors may also be constituted by serum stimulatory autoantibodies activating the PDGFR. This hypothesis was based not only on previous studies (11,13,14) reporting the presence in SSc patients' serum of anti-PDGFR antibodies carrying agonistic activity towards fibroblasts *in vitro*, but also on additional studies by other groups highlighting the central role *in vivo* of PDGF/PDGFR signalling in fibrosis and SSc (31,32). Hence, skin-humanized mice were engrafted with bioengeneered skin prepared from healthy donors and injected *in vivo* with IgG purified from serum of either SSc patients or healthy controls. To avoid biases due to the different clinical features of donors, two IgG pools were made, one from eight SSc patients, the other one from eight HC, using the same amount of IgG from each donor. Prior to pooling, even low levels of contaminating TGFβ and PDGF-BB in individual IgG preparations was excluded by western blots of high concentrations of IgG with specific antibodies to PDGF and TGFβ. Moreover, the presence of agonistic anti-PDGFR antibodies able to induce ROS and collagen were detected in 8/8 SSc-IgG preparation and in none of HC-IgG (12). Recall that the same IgG preparations were unable to induce ROS in PDGFR-/- fibroblasts (11). Unlike the duplicate grafts injected with HC-IgG, those injected with SSc-IgG displayed significant collagen accumulation, and the explanted fibroblasts exhibited higher than

normal levels of Ha-Ras, pERK-1/2, ROS, and COL1A2. Thus, SSc-IgG-induced dermal fibrosis was associated *in vivo* with activation of the same cell signaling loop previously reported to sustain the phenotype of SSc fibroblasts *in vitro* (6). These results demonstrate that SSc-IgG can activate healthy fibroblasts *in vivo* in a manner that faithfully replicates the histological and molecular features of SSc skin.

To demonstrate that dermal fibrosis was specifically induced *in vivo* by SSc-IgG via PDGFR activation, the experiments were repeated after treating the mice with nilotinib, a potent, second-generation TKI. Oral administration of nilotinib to mice significantly inhibited the increase of type I collagen dermal deposition induced by SSc-IgG.

However, Nilotinib may target other nonkinase substrates (28) and the inhibitory effects seen in our model may not be ascribed to the inhibition of PDGFR signaling. Since we cloned antibodies that induce collagen or ROS selectively through PDGFR (14), we tested one of these antibodies in the human skin engineered model and we find that its pro-fibrotic action is undistinguishable from the activity of SSc-IgG, strongly arguing that the pro-fibrotic activity of SSc-IgG is essentially mediated by PDGFR.

In addition to establishing the informative value of this novel chimerical mouse-human SSc model to study fibroblast activation *in vivo*, our data provided information also on the vascular counterpart alterations. Vascular damage, primarily involving the small vessels, is likely an early event in SSc, preceding dermal fibrosis and characterized, in the first phases of SSc, by perivascular infiltrate of mononuclear immune cells in the vessel wall, obliterative microvascular lesions, and rarefaction of capillaries (33). Besides directly promoting fibrosis, PDGFR signaling could also be involved in the

vasculopathy seen in SSc. In fact, PDGFR is up-regulated on microvascular pericytes in early-stage SSc skin biopsies (34) and increased PDGFR activity and pericyte activation in SSc may cause capillary occlusion and regression independently of fibroblast activation. Our data demonstrated that SSc-IgG and agonistic anti PDGFR monoclonal antibody induced a significant reduction of the dermal vessel count, which was prevented by SSc-IgG administration together with nilotinib. Since in our model: i) the vasculature is entirely murine (17), ii) endothelial cells do not express PDGF receptor (35); and iii) the homology between mouse and human PDGFR is 85% (36), it is likely that the observed vessel desertification was secondary to dermal fibrosis and not primarily caused by the anti-PDGFR activity of SSc-IgG, which would require a mouse model characterized by the ubiquitous expression of human PDGFR in order to be formally demonstrated.

Moreover, it must be noted that dermal fibrosis in these novel skin humanized models of SSc is not sustained by any inflammatory response of the skin tissue, further confirming that the microvasculature damage observed in our mice is not dependent upon inflammatory mechanisms, likely involved in the earliest phases of SSc.

Finally, our data add on previous studies (37-39) reporting TKI as a possible therapeutic strategy against SSc, and demonstrate that these chimerical models of SSc fibrosis provide a novel tool to evaluate the efficacy of existing and experimental therapies for scleroderma.

REFERENCES

1. Varga J, Abraham D. Systemic sclerosis: a prototypic multisystem fibrotic disorder. J Clin Invest 2007; 117:557-567.

2. Gabrielli A, Avvedimento EV, Krieg T. Scleroderma. N Engl J Med 2009; 360:1989-2003.

3. Varga J, Bashey RI. Regulation of connective tissue synthesis in systemic sclerosis. Int Rev Immunol 1995; 12:187-199.

4. Trojanowska M. Molecular aspects of scleroderma. Front Biosci 2002; 7:d608-618.

5. Krieg T, Perlish JS, Mauch C, Fleischmajer R. Collagen synthesis by scleroderma fibroblasts. Ann N Y Acad Sci 1985; 460:375-386.

6. Svegliati S, Cancello R, Sambo P, Luchetti M, Paroncini P, Orlandini G, et al. Platelet-derived growth factor and reactive oxygen species (ROS) regulate Ras protein levels in primary human fibroblasts via ERK1/2. Amplification of ROS and Ras in systemic sclerosis fibroblasts. J Biol Chem 2005; 280:36474-36482.

7. Gabrielli A, Svegliati S, Moroncini G, Amico D. New insights into the role of oxidative stress in scleroderma fibrosis. Open Rheumatol J 2012; 6:87-95.

8. Smaldone S, Olivieri J, Gusella GL, Moroncini G, Gabrielli A, Ramirez F. Ha-Ras stabilization mediates pro-fibrotic signals in dermal fibroblasts. Fibrogenesis Tissue Repair 2011; 4:8.

9. Leask A, Abraham DJ. TGF-beta signaling and the fibrotic response. Faseb J 2004; 18:816-827.

10. Bonner JC. Regulation of PDGF and its receptors in fibrotic diseases. Cytokine Growth Factor Rev 2004; 15:255-273.

11. Baroni SS, Santillo M, Bevilacqua F, Luchetti M, Spadoni T, Mancini M, et al. Stimulatory autoantibodies to the PDGF receptor in systemic sclerosis. N Engl J Med 2006; 354:2667-2676.

12. Cuccioloni, M., Moroncini, G., Mozzicafreddo, M., Pozniak, K.N., and Nacci, G. 2013. Biosensor-based binding assay for Platelet-Derived Growth Factor Receptor-alpha autoantibodies in human serum. J Anal Bioanal Tech 2013; S 7:010.

13. Svegliati S, Marrone G, Pezone A, Spadoni T, Grieco A, Moroncini G, et al. Oxidative DNA damage induces the ATM-mediated transcriptional suppression of the Wnt inhibitor WIF-1 in systemic sclerosis and fibrosis. Sci Signal 2014; 7:ra84.

14. Moroncini G, Grieco A, Nacci G, Chiara Paolini C, Cecilia Tonnini C, Pozniak KN, et al Epitope specificity determines pathogenicity and detectability of anti-PDGFRα autoantibodies in systemic sclerosis Arthritis Rheumatol 2015*;* 67: 1891–1903.

15. Llames SG, Del Rio M, Larcher F, Garcia E, Garcia M, Escamez MJ, et al Human plasma as a dermal scaffold for the generation of a completely autologous bioengineered skin. Transplantation 2004; 77:350-355.

16. Rheinwald JG, Green H. Serial cultivation of strains of human epidermal keratinocytes: the formation of keratinizing colonies from single cells. Cell 1975; 6:331-343.

17. Guerrero-Aspizua S, Garcia M, Murillas R, Retamosa L, Illera N, Duarte B, et al. Development of a bioengineered skin-humanized mouse model for psoriasis: dissecting epidermal-lymphocyte interacting pathways. Am J Pathol 2010; 177:3112-3124.

18. Escamez MJ, Garcia M, Larcher F, Meana A, Munoz E, Jorcano JL, et al. An in vivo model of wound healing in genetically modified skin-humanized mice. J Invest Dermatol 2004; 123:1182-1191.

19. Larcher F, Del Rio M, Serrano F, Segovia JC, Ramirez A, Meana A, et al. A cutaneous gene therapy approach to human leptin deficiencies: correction of the murine ob/ob phenotype using leptin-targeted keratinocyte grafts. Faseb J 2001; 15:1529-1538.

20. Carretero M, Escamez MJ, Prada F, Mirones I, Garcia M, Holguin A, et al. Skin gene therapy for acquired and inherited disorders. Histol Histopathol 2006; 21:1233-1247.

21. Warrick E, Garcia M, Chagnoleau C, Chevallier O, Bergoglio V, Sartori D, et al. Preclinical corrective gene transfer in xeroderma pigmentosum human skin stem cells. Mol Ther 2012; 20:798-807.

22. Serrano F, Del Rio M, Larcher F, Garcia M., Muñoz E, Escamez MJ, et al. A Comparison of Targeting Performance of Oncoretroviral versus Lentiviral Vectors on Human Keratinocytes. Hum Gene Ther 2003, 14, 1-7.

23. Andrae J, gallini R, Betsholtz C. Role of platelet-derived growth factors in physiology and medicine. Genes Dev 2008; 22: 1276-312

24. Manley PW, Drueckes P, Fendrich G, Furet P, Liebetanz J, Martiny-Baron G, et al.. Extended kinase profile and properties of the protein kinase inhibitor nilotinib. Biochim Biophys Acta 2010; 1804:445-453.

25. Jimenez SA, Hitraya E, Varga J. Pathogenesis of scleroderma. Collagen. Rheum Dis Clin North Am 1996; 22: 647-674.

26. Walters R, Pulitzer M, Kamino H. Elastic fiber pattern in scleroderma/morphea. J. Cutan Pathol 2009; 36:952-57.

27. Iwamoto N, Distler JH, Distler O Tyrosine kinase inhibitors in the treatment of systemic sclerosis: from animal models to clinical trials.Curr Rheumatol Rep. 2011;13: 21-7.

28. Rix U, Hantschel O, Dürnberger G, Remsing Rix LL, Planyavsky M, Fernbach NV et al. Chemical proteomic profiles of the BCR-ABL inhibitors imatinib, nilotinib, and dasatinib reveal novel kinase and nonkinase targets. Blood 2007; 110:4055-63

29. Asano Y, Sato S. Animal models of scleroderma: current state and recent development. Curr Rheumatol Rep 2013; 15:382.

30. Beyer C, Schett G, Distler O, Distler JHW. Animal models of Systemic sclerosis. Prospects and limitations. Arthritis Rheum 2010; 62: 2831-2844

31. Olson LE, Soriano P. Increased PDGFRalpha activation disrupts connective tissue development and drives systemic fibrosis. Dev Cell 2009; 16:303-313.

32. Iwayama T, Olson LE. Involvement of PDGF in fibrosis and scleroderma: recent insights from animal models and potential therapeutic opportunities. Curr Rheumatol Rep 2013; 15:304.

33. Muller-Ladner U, Distler O, Ibba-Manneschi L, Neumann E, Gay S. Mechanisms of vascular damage in systemic sclerosis. Autoimmunity 2009; 42:587-595.

34. Rajkumar VS, Sundberg C, Abraham DJ, Rubin K, Black, CM. Activation of microvascular pericytes in autoimmune Raynaud's phenomenon and systemic sclerosis. Arthritis Rheum 1999; 42:930-941.

35. Heldin CH, Westermark B, Wasteson A Specific receptors for platelet-derived growth factors on cells derived from connective tissue and glia. Proc Natl Acad Sci U S A. 1981; 78:3664-8.

36. Claesson-Welsh L, Eriksson A, Morén A, Severinsson L, Ek B, Ostman A et al cDNA cloning and expression of a human platelet-derived growth factor (PDGF) receptor specific for B-chain-containing PDGF molecules. Mol Cell Biol. 1988; 8:3476-86.

37. Distler JH, Distler O. Intracellular tyrosine kinases as novel targets for anti-fibrotic therapy in systemic sclerosis. Rheumatology (Oxford) 2008; 47 Suppl 5:v10-11.

38. Bournia VK, Evangelou K, Sfikakis PP. Therapeutic inhibition of tyrosine kinases in systemic sclerosis: a review of published experience on the first 108 patients treated with imatinib. Semin Arthritis Rheum 2012; 42:377-390

39. Fraticelli P, Gabrielli B, Pomponio G, Valentini G, Bosello S, Riboldi P, et al. Low-dose Oral Imatinib in the Treatment of Systemic Sclerosis Interstitial Lung Disease unresponsive to cyclophosphamide. A Phase II Pilot Study. Arthritis Res Therapy 2014; 16:R144.

,

Fig. 1 Histopathological and molecular analysis of scleroderma skin-humanized mice

A, Haematoxylin-eosin staining (left panels magnification 200X) of healthy control (HC,top) and scleroderma (SSc, bottom) regenerated skins and picrosirius red staining (right panels magnification 40X) 8 weeks after grafting to immunodeficient mice. Representative images of 6 skin grafts are shown. **B,** Picrosirius red positive areas in SSc skin grafts (n=6), as percentage of the same staining in HC skin grafts (n=6), 8 weeks after engrafting. Data are means ± SD; *= p<0.001. **C,** Immunoprecipitation of Ha-Ras and immuno-blot for pERK-1/2 in lysates of fibroblasts grown from skin biopsies (SB), and in fibroblasts grown from 8-week old regenerated skin grafts (SG) from 2 HC and 2 SSc patients**.** Blots are representative of 3 independent experiments with 6 distinct fibroblast cell lines. Densitometric analysis (lower panel) of the blots. Data are means ± SD; *= p<.0.01. **D,** Left, ROS production from SB fibroblasts of SSc patients (n=3) and HC (n=3) and from SG derived fibroblasts from SSc (n=6) and HC (n=6) obtained at the same time point of Panel C. Data are means ± SD; *= p< 0.01. Right, COLA1A2 expression in SB and SG fibroblasts obtained as in panel C. Data are means ± SD; * = p<0.01.

Fig 2. Histopathological and molecular analysis of healthy control skin grafts injected with SSc-IgG and HC-IgG

A, Left, picrosirius staining of a HC skin graft 2 weeks after the first injection with PBS HC-IgG or SSc-IgG. Representative images of 3 grafts with each treatment are shown. Original magnification, X 200. Right, picrosirius positive areas in HC- skin grafts injected with SSc-IgG (n= 3) or HC-IgG (n=3), as percentage of the same staining in HC-skin grafts treated with PBS (n=3) 2 weeks after the first treatment. Data are means ± SD; *= p< 0.001**. B,** Ha-Ras and pERK-1/2 in lysates of fibroblasts grown from biopsies of HC skin grafts injected with PBS, HC-IgG, or SSc-IgG. Blots

are representative of 3 independent experiments with 3 distinct fibroblast cell lines from each treatment group at the same time point of panel D. (lower panel) densitometric analysis of the blots. Data are means ± SD; * = p<0.01**. C,** ROS production (left) and COL1A2 gene expression (right) of fibroblasts derived from biopsies as in B. Data are means ± SD of 3 independent experiments with 3 distinct cell lines from each treatment group. ***** = p<0.01. **D**, Left, Representative images of CD31 positive vessels of a HC skin grafts treated as in A. Original magnification, X 200. Right, CD31 positive vessels in HC skin grafts treated as in A. Data are means ± SD of 3 grafts of each treatment group analyzed in 3 randomly chosen high power field. * = p<0.01.

Fig 3. Partial amelioration of SSc phenotype in HC skin grafts injected with SSc-IgG after nilotinib administration

A, Haematoxylin-eosin staining of HC skin grafts which received HC-IgG and vehicle, HC-IgG plus nilotinib**,** SSc-IgG and vehicle, or SSc-IgG plus nilotinib. Representative images of 4 skin grafts of each experimental group are shown. Original magnification, X 200**. B**, Dermal thickness of HC-skin grafts (n=4 in each group) treated as in A. Data are means ± SD fold increase in skin thickness compared to vehicle treated mice. * = p <0.05**. C,** Real-time PCR analysis of COL1A2 in skin grafts of Panel A. Data are means ± SD fold increase in expression compared to that of vehicle treated mice. * = p < 0.01. **D,** Left, Representative tissue sections of 4 skin grafts treated as shown, stained with picrosirius red and observed under polarized light**.** Right, Quantification of picrosirius positive areas of skin grafts as percentage of the same staining in skin grafts of HC- IgG and vehicle treated mice. Data are means ± SD; * = p<0.01**.**

Fig 4 Nilotinib administration prevented the reduction of CD 31 positive vessels induced by the SSc-IgG.

A, Human regenerated skin grafts from mice treated as described in Fig 3 were evaluated for CD 31 positive vessels. Representative images of 4 skin grafts of each experimental group are shown. Original magnification, X 200. **B,** Number of CD 31 positive vessels in skin grafts shown in Panel A. Data are means ± SD of 4 grafts of each experimental group. Each graft was analyzed in 3 randomly chosen high power fields. * = $p < 0.01$

Fig 5. SSc phenotype in HC skin grafts injected with human monoclonal antibodies targeting PDGF receptor

A, Left, picrosirius red staining of a HC skin graft 2 weeks after the injection with PBS, V_HPAM-V_κ13B8, and V_HPAM-V_κ16F4 anti PDGFR monoclonal antibodies (see text for explanation). Representative images of 3 grafts with each experimental treatment are shown. Original magnification, X200. Right, Quantification of picrosirius red positive areas in HC- skin grafts injected with the above monoclonal anti PDGFR monoclonal antibodies (n=3 in each experimental group) as percentage of the same staining in HC-skin grafts treated with PBS (n=3) 2 weeks after the treatment. Data are means ± SD; *= $p < 0.001$**. B,** Real-time PCR analysis of COL1A2 in skin grafts of Panel A. Data are means ± SD fold increase in expression compared to that of PBS treated mice. * = $p < 0.01$. **C,** Left**,** CD31 positive vessels in HC skin graft skin grafts from mice treated as in A. Representative images of 3 skin grafts of each experimental group are shown. Original magnification, X 200. Right, Number of CD31 positive vessels in skin

grafts shown on the left. Data are means ± SD of 3 grafts of each experimental group analyzed in 3 randomly chosen high power fields. * = p< 0.01

Supplementary Fig.1. Validation in vitro of purified immunoglobulins from scleroderma patients (SSc-IgG) before the injection in the regenerated human skin in vivo.

A. FACS analyses of platelet-derived growth factor receptor (PDGFR) alpha (PDGFRα) and –beta (PDGFRβ) expression in normal human fibroblasts either untreated or transfected with short- hairpin-RNA (shRNA) anti-PDGFRα and anti-PDGFRβ retroviral vectors. **B,** Immunoblot analyses of PDFGR expression in normal human fibroblasts transfected as in A. **C.** Immunoprecipitation of Ha-Ras and real-time PCR analysis of COL1A2 **(D)** in normal human fibroblasts stimulated with normal IgG (HC-IgG) or SSc-IgG (SSc-IgG), in the presence or absence of anti-PDGFRα and anti-PDGFRβ shRNAs. Data are means ± SD of 3 independent experiments with 3 distinct fibroblast cell lines. *= p< 0.01.

AUTHOR CONTRIBUTIONS

All authors were involved in drafting the article or revising it critically for important intellectual content, and all authors approved the final version. Drs. Luchetti and Gabrielli had full access to all of the data of the study and take responsibility for the integrity of the data and the accuracy of the data analysis.

Study conception and design: Luchetti, Larcher, Del Rio, Avvedimento and Gabrielli.

Acquisition of data: Escamez, Svegliati Baroni, Spadoni, Grieco, Paolini, Moroncini.

Analysis and interpretation of data: Luchetti, Moroncini, Svegliati, Avvedimento, Larcher, Del Rio, Gabrielli

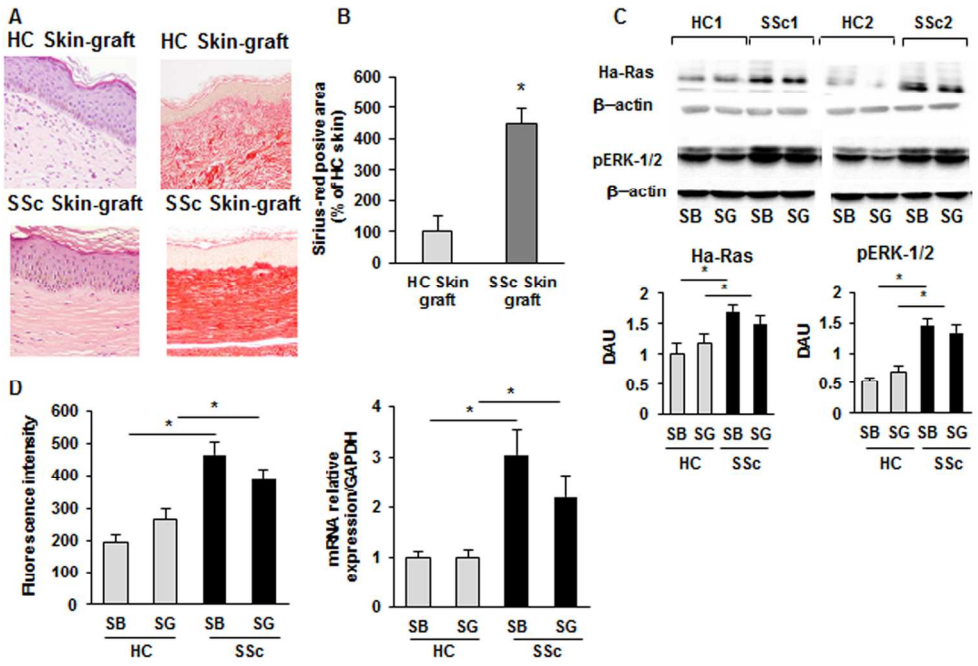

163x109mm (300 x 300 DPI)

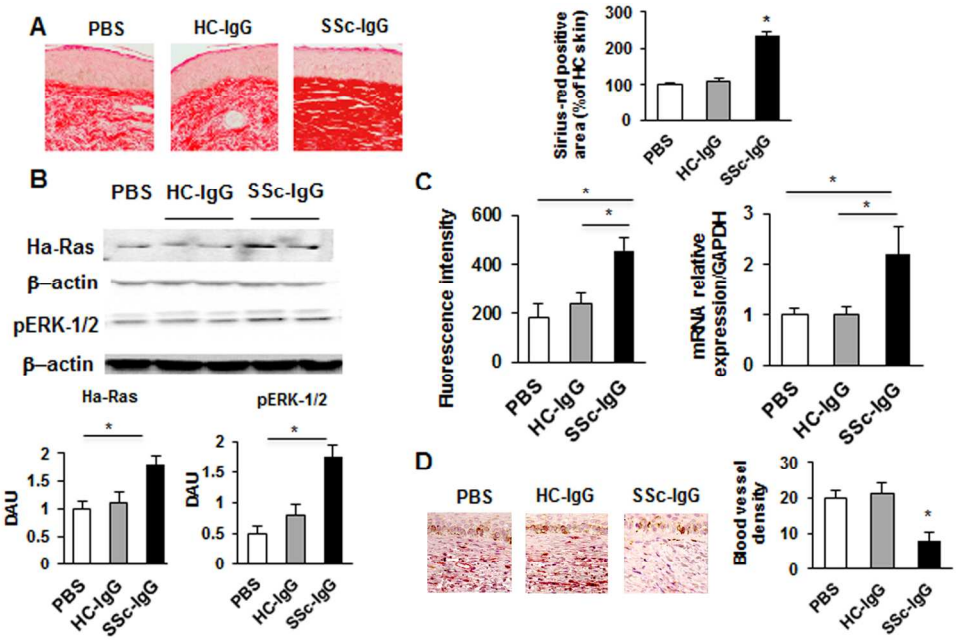

170x110mm (300 x 300 DPI)

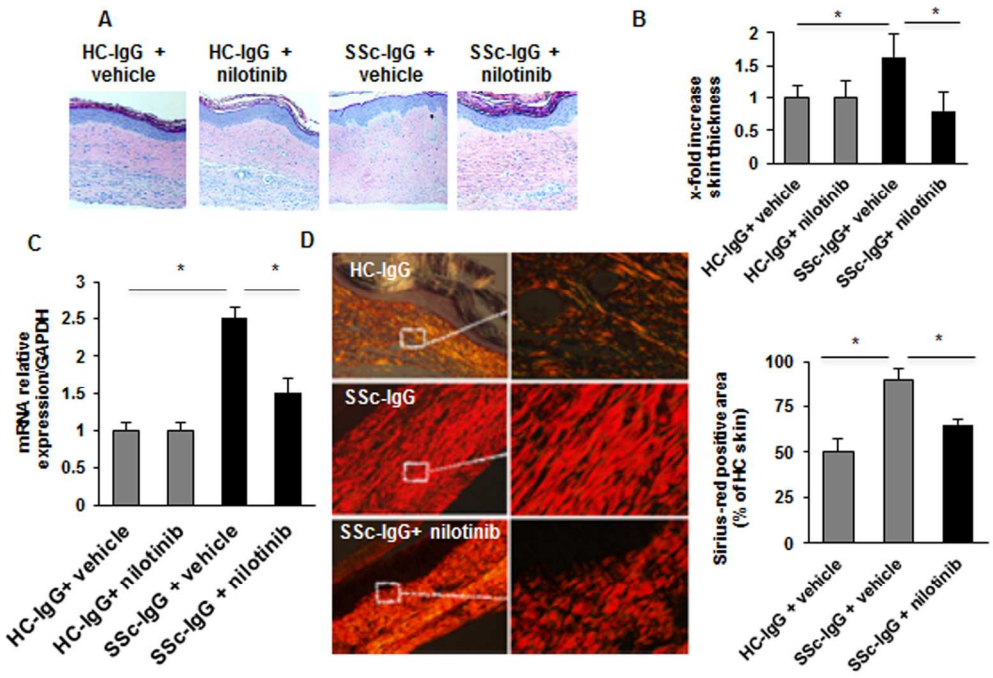

160x109mm (300 x 300 DPI)

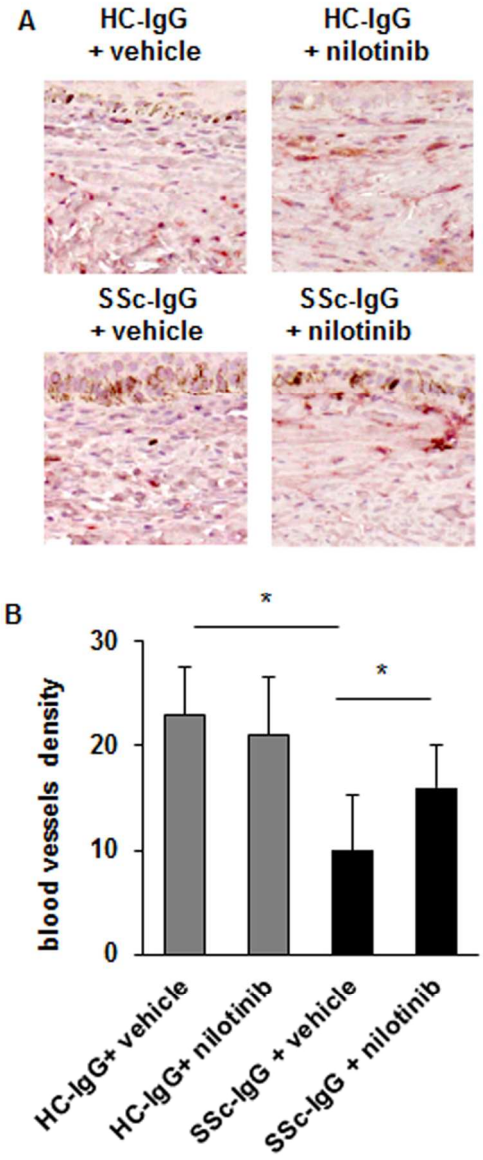

80x188mm (300 x 300 DPI)

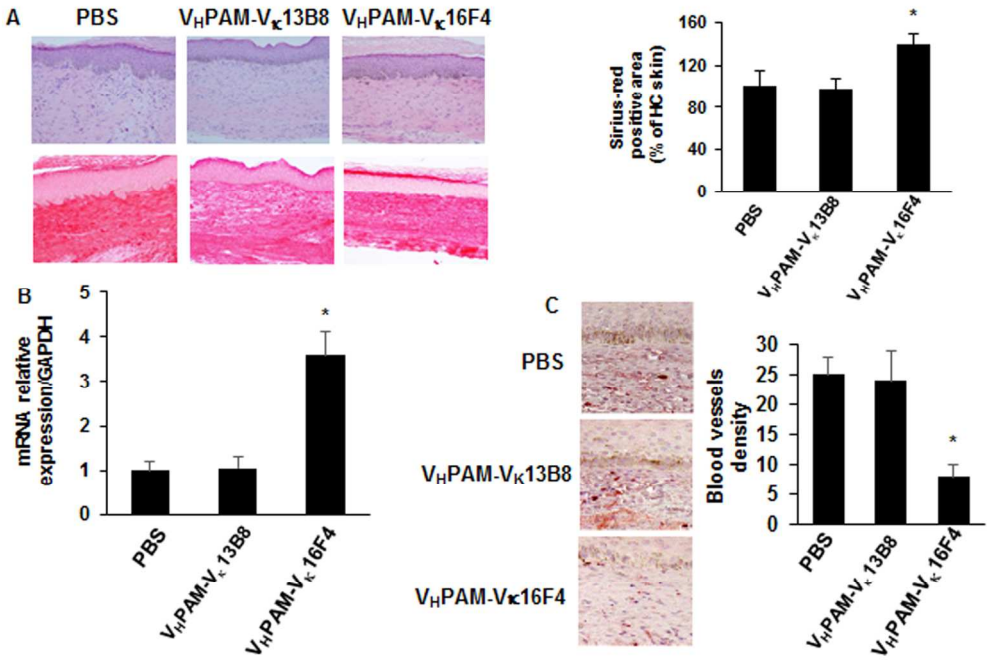

161x109mm (300 x 300 DPI)